POINT SPREAD FUNCTIONS FOR SDO/AIA

Bala Poduval
Southwest Research Institute, Boulder, CO
In collaboration with
C. E. Deforest (SwRI),
J. T. Schmelz and S. Pathak (Univ of Tennesse)

Point Spread Function

- Optical telescopes convolve their images with a PSF that describes the response of the optical system to a point source, resulting in the blurring of the images.
- PSF includes: core elements that describe the focusing performance of telescope; broad elements representing scattering of light in the telescope.

AIA - Instrument

- 7 EUV: 94, 131, 171, 193, 211, 304, 335 Å.
- 2 FUV and one visible.
- pixel size : 0.6" (12μm), spatial resolution:1.5", temporal resolution:10-12 sec.,

  CCD : 4096 x 4096
- Filters: entrance, focal plane – block off-band light.

FILTERS

- are mounted on square mesh with spacing: 360 µm; thickness of mesh bars: 29-33 µm.
- Focal plane filter: produces a faint shadow in the focal plane; flat fielding can remove it.
- Entrance filter: acts as two-dimensional grating; causes Fraunhoffer diffraction of incoming EUV light.

SDO/AIA filters are similar to those of TRACE.

ENTRANCE FILTER

- The mesh consists of two segments: 40 and 50° orientations relative to the focal plane.
- Eight-armed diffraction pattern best seen in high contrast images as in solar flares.
- Diffraction pattern varies with
- wavelength of incoming light,
- thickness of the mesh-bars and the spacing between them,
- and the orientations of the mesh segments.

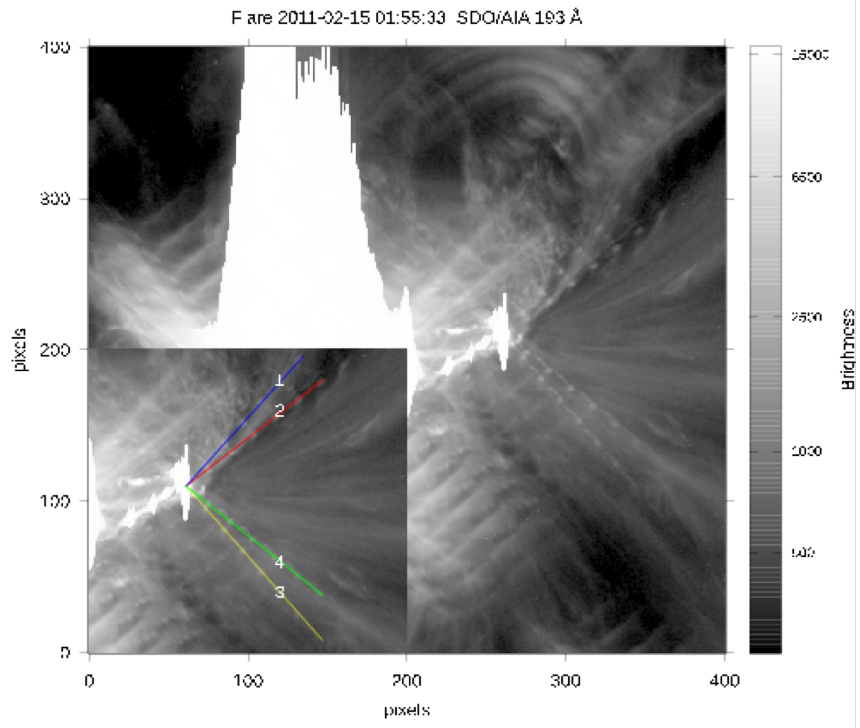

MODEL PSF

In addition to diffraction, SDO/AIA images show a smooth, extended scattering profile, in form of diffuse brightness.

PSF we modelled has two components: (1) a directly measured diffraction kernel; (2) a fitted, isotropic scattering profile (DeForest, et al., *ApJ*, **690**, 1264-1271, 2009), consisting of a Gaussian truncated Lorentzian and a shoulder Gaussian.

Other artifacts: CCD overflow or saturation, or the vertical stripes seen in images can not be described by a simple convolution, and therefore, will not be removed by deconvolution by the PSF.

Model PSF

- $$PSF = e^{-4\ln(2)r^2/\sigma^2} + D(r,\theta) + \propto \frac{e^{-4\ln(2)r^2/\sigma_t^2}}{(r^2\,\omega^{-2}) + 1} + \beta\, e^{-4\ln(2)r^2/\sigma_s^2} \qquad (1)$$

  r: distance in the image plane; D(r, θ): diffraction pattern; α, β: relative strengths of Lorentzian and shoulder Gaussian; ω: width of Lorentzian; σ, σ_t, σ_s: full-widths at half maximum of the central core of the PSF, and the truncating and shoulder Gaussians.

DIFFRACTION

- Fraunhoffer diffraction: for ideal, uniformly spaced mesh, the distance d_m, of the principal maxima of the diffraction pattern from the center (zeroth order) is:

$$d(m) = m\frac{\lambda}{a} \qquad (2)$$

m: the diffraction order; λ: the wavelength of the light used; a: the distance between the mesh bars.

Diffraction

- Intensity of the zeroth order:

$$I_0 = I_m \left(\frac{\sin\left(\frac{m\pi b}{a}\right)}{m\pi b/a} \right)^{-2} \quad (3)$$

I_0, I_m: intensities of zeroth order, and order *m;*

b: the width of the openings.

Extraction of PSFs

- The diffraction effects are modelled using the geometry of the pattern and intensities at the principal maxima, measured directly from the pattern visible around solar flares.
- The diffuse components of the PSF are fitted using a forward-modelling fit process operating on lunar eclipse images containing the lunar limb.

SOLAR FLARE DATA

February 15, 2011, caused by Sunspot group 1158.

- Strong flares cause CCD saturation of the flaring area. This obscures the first few orders of the diffraction pattern.
- If the flare is weak, then the pattern blends with the background and the diffraction orders become indistinguishable.
- The X2-class flare peaked at 01:56UT; we selected images between 01:55:33 and 01:55:52 UT.

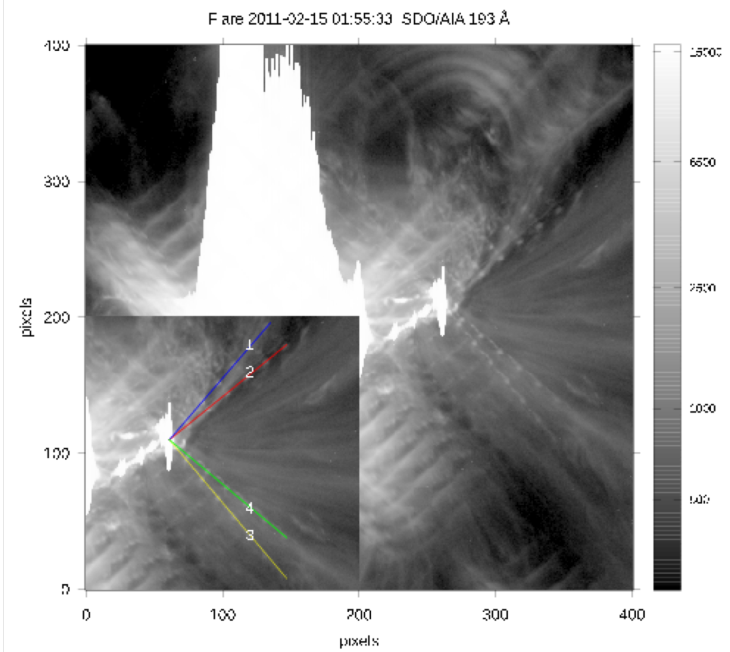

Lunar Occultation Data

- SDO/AIA observed a lunar transit during March 4, 2011.
- The instrument's image stabilization system (ISS) was on; so there was little or no blurring.
- Selected images: 13:00:01 - 13:04:05 UT.
- Effects of stray light (as diffuse brightness inside the lunar disc) and diffraction (as dark and bright ridges near the active region) are clearly visible.

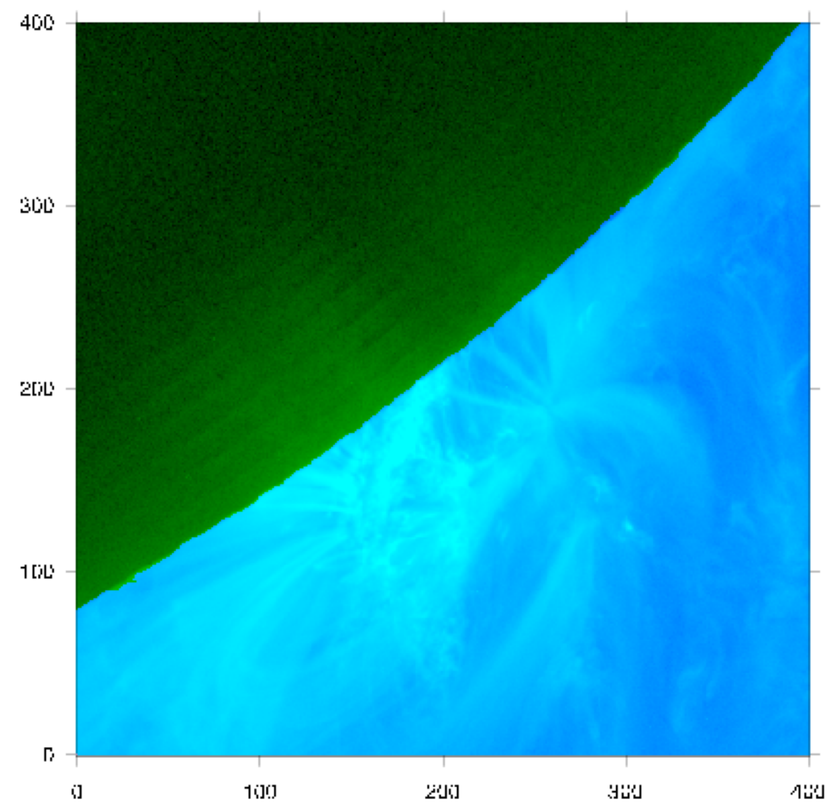

AIA DATA

- Level-1 data available in JSOC (http://jsoc.stanford.edu/ajax/lookdata.html).
- Level-1 data: processed from Level-0 and: corrected for over scan rows and columns; dark-currents removed and flat-fielded; have bad pixels replaced by interpolated values and despiked; are flipped to have the north pole at the top of each image; metadata updated to include instrument roll angle, the camera gain, the effective area, and alignment information (Lemen et al., 2012, Boerner et al., 2012).
- Level-1 data are 32-bit floating point numbers.

Modelling the Diffraction Pattern

- Four arms to measure geometry of the pattern and intensities of the principal maxima; first six or seven orders - to model the diffraction pattern.
- Angles of rotation to make the arms parallel to the X-axis - orientations.
- Measured the coordinates of core and centers (visually determined) of the principal maxima - spacings between diffraction orders.
- Spacings for a given wavelength were not uniform, but differed by 1-2 pixels.

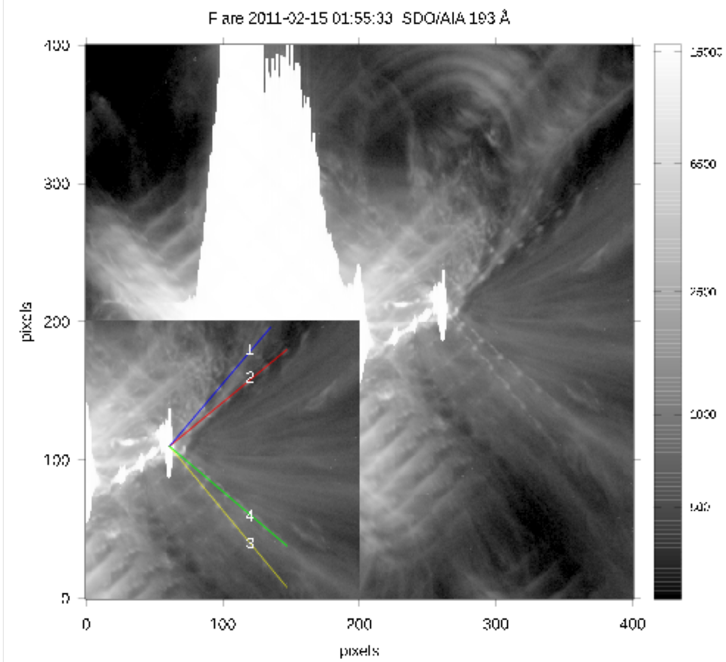

MODELLING THE DIFFRACTION PATTERN

- Zeroth order intensity (at the center of the pattern) - measured from image.
- CCD saturation by the flare caused ambiguity.
- Discrepancies: measured locations of principal maxima did not always coincide with local maxima, but differed by 1-2 pixels: presence of non-uniform background and photon noise in the bright spots, or unknown distortion in the instrument related to flare response.
- CCD saturation causes additional background near higher orders.

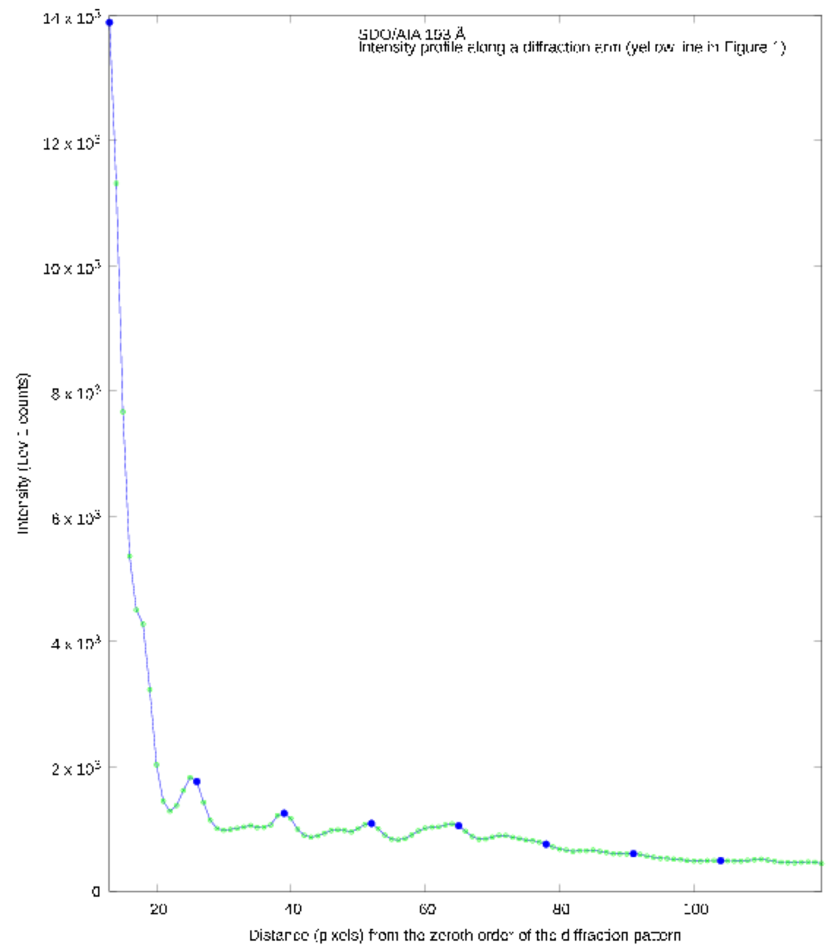

Intensities at the Principal Maxima

Instead of taking the direct image values at each bright spots, we computed:

- average intensity, I_{peak}, in a 3X3 (pixels) area;
- average intensities of preceding (I_{prec}) and succeeding (I_{succ}) troughs, and their mean, I_{trough}.

Subtracted I_{trough} from I_{peak}.

Using the geometry and intensities, we constructed the diffraction pattern on an 801x801 pixel grid.

Tried 1201x1201, but no significant improvement; 801 sufficiently covered the observed effects.

NEED FOR THEORETICAL COMPUTATIONS

- • CCD saturation causes ambiguities in the measurements of intensities at the principal maxima, particularly the lower orders, not to mention the zeroth order.
- Computed the intensities using:

$$I_0 = I_m \left(\frac{\sin\left(\frac{m\pi b}{a}\right)}{m\pi b/a} \right)^{-2}$$

- Obtained best-fit values for *b/a* for each wavelength; 0.892 for 211 Å (Lin et al., *Solar Phys.*, **198**, 385-395).

Need for Theoretical Computations

- The theoretical values of intensities were significantly different from the measured values.
- The theoretical diffraction pattern better explained large-scale stray-light features such as the ridges within the lunar limb than the measured diffraction pattern.
- The theoretical values were used to optimize the spacings and orientations and compute the diffraction kernel of the model PSF.

Fitted Geometry of the Diffraction Pattern

λ Å	Spacings (pixels)				Orientations (˚)			
	Arm 1	Arm 2	Arm 3	Arm 4	Arm 1	Arm 2	Arm 3	Arm 4
94	8.867	8.867	8.867	8.867	39.767	49.967	-39.833	-49.963
131	12.3567	12.3567	12.3567	12.3567	39.767	49.967	-39.833	-49.963
171	16.277	16.267	16.281	16.237	40.057	49.917	-39.733	-49.963
193	18.361	18.361	18.361	18.361	39.967	50.167	-39.833	-49.963
211	19.87	19.87	19.87	19.87	39.97	49.97	-39.93	-49.963
304	28.867	28.867	28.867	28.867	39.867	49.967	-40.233	-49.963
335	31.867	31.867	31.867	31.867	39.767	49.967	-39.833	-49.963

Fitted diffraction pattern

This SDO/AIA image was taken in 211 Å at 01:55:28 UT on February 15, 2011.

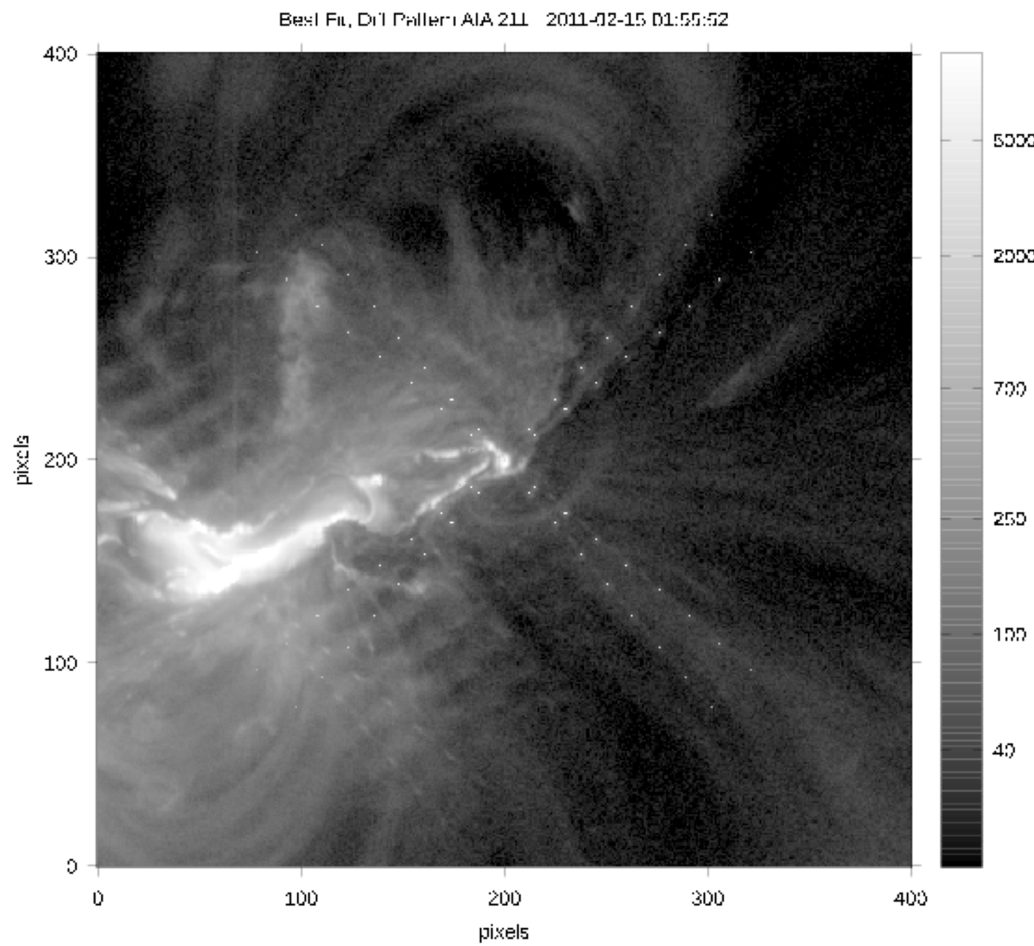

FITTING THE MODEL PSF - REFERENCE IMAGE

- PSF computed on an 801 x 801 pixel grid.
- Used the darkness in the occulting lunar disc to constrain the fitting procedure.
- Mask: determined the lunar limb; 1201x1201 pixel with zeros within the lunar disc and ones outside the disc.
- Reference image: 1201x1201 pixel image slice around the active region; multiplied by the mask.

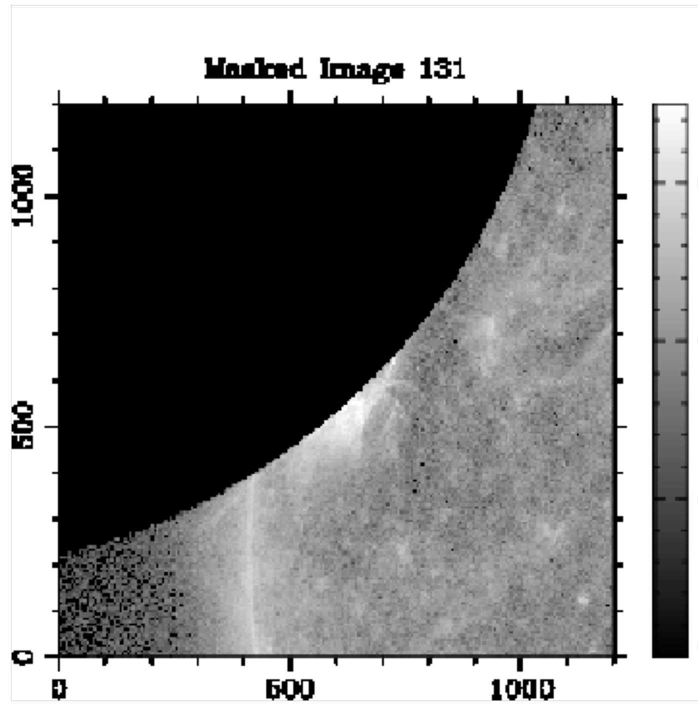

Final PSF

- Starting with an initial set of guess values for the parameters in the model PSF, we obtained a trial PSF.
- The reference image was convolved with the trial PSF to get a test image.
- Optimize the fitting: a heuristic that minimizes the RMS difference between the values inside the occulted region of the original and test images.
- The final PSF was computed using the best-fit values for all the parameters.

Best-fit values of the PSF parameters

λ (Å)	α	ω pixels	β	σ_s pixels
94	1.256e-3	2.1	3.0e-2	1.721
131	2.0e-2	0.5	1.0e-3	2.6
171	1.76265	0.10122	1.2e-1	1.35
193	4.0e-4	3.9	8.0e-2	1.64
211	4.2e-4	3.6	2.35e-2	2.1
304	2.0e-2	0.2	1.0e-2	2.0
335	2.78e-4	1.90269	2.3678e-2	1.5924

$$PSF = e^{-4\ln(2)r^2/\sigma^2} + D(r,\theta) + \propto \frac{e^{-4\ln(2)r^2/\sigma_t^2}}{(r^2\,\omega^{-2})+1} + \beta\, e^{-4\ln(2)r^2/\sigma_s^2}$$

σ, the FWHM of the core was kept at 0.2 pixels (0.12 ”).

σ_t, the width of the truncating Gaussian, was kept 798 for all the wavelengths since that is the maximum possible for a grid size of 801 x 801.

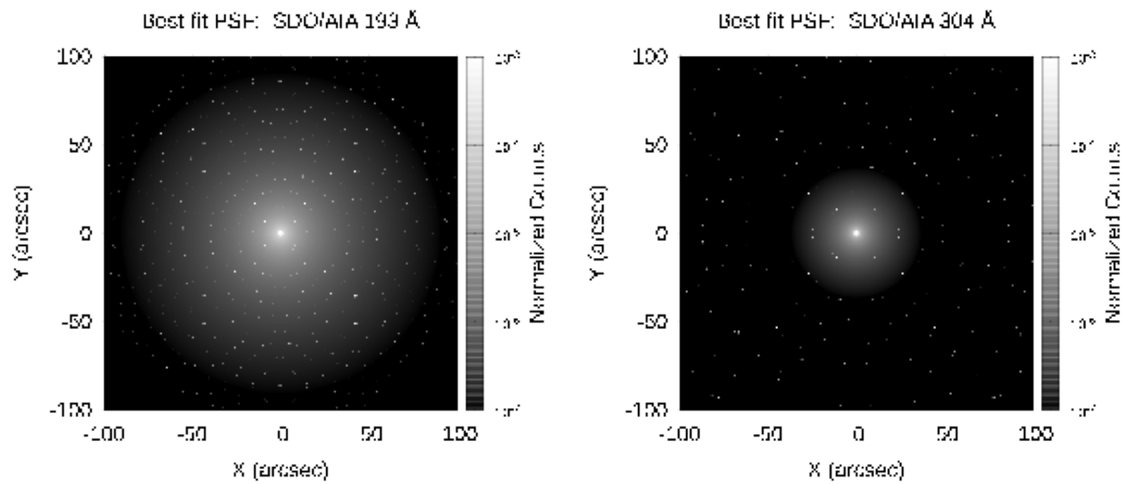

The PSFs computed for 171 and 304 Å.

The PSFs are normalized to unity and are plotted on a log scale.

Comparison – Original & Deconvolved

EUV wavelengths: 94, 131, 304 and 335 Å

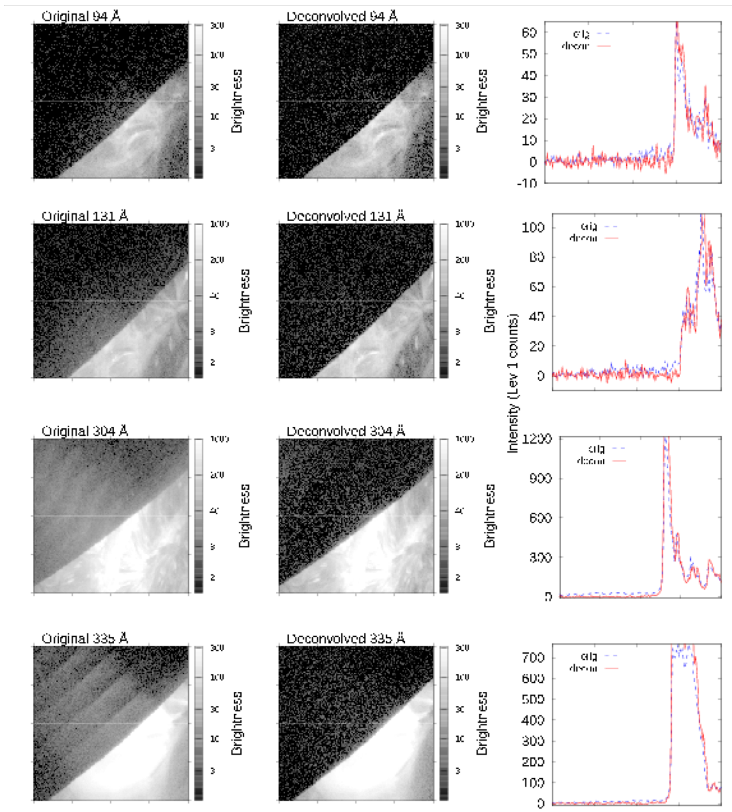

EUV wavelengths: 171, 193 and 211 Å.

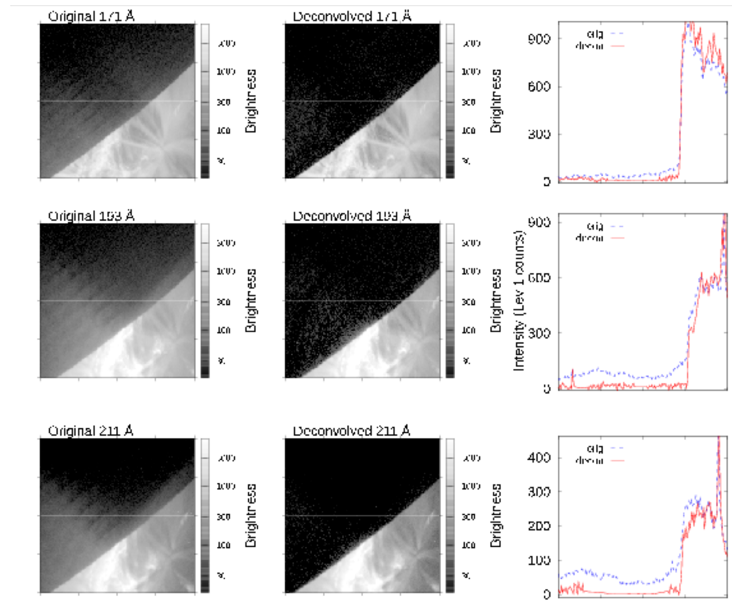

ENCIRCLED ENERGY

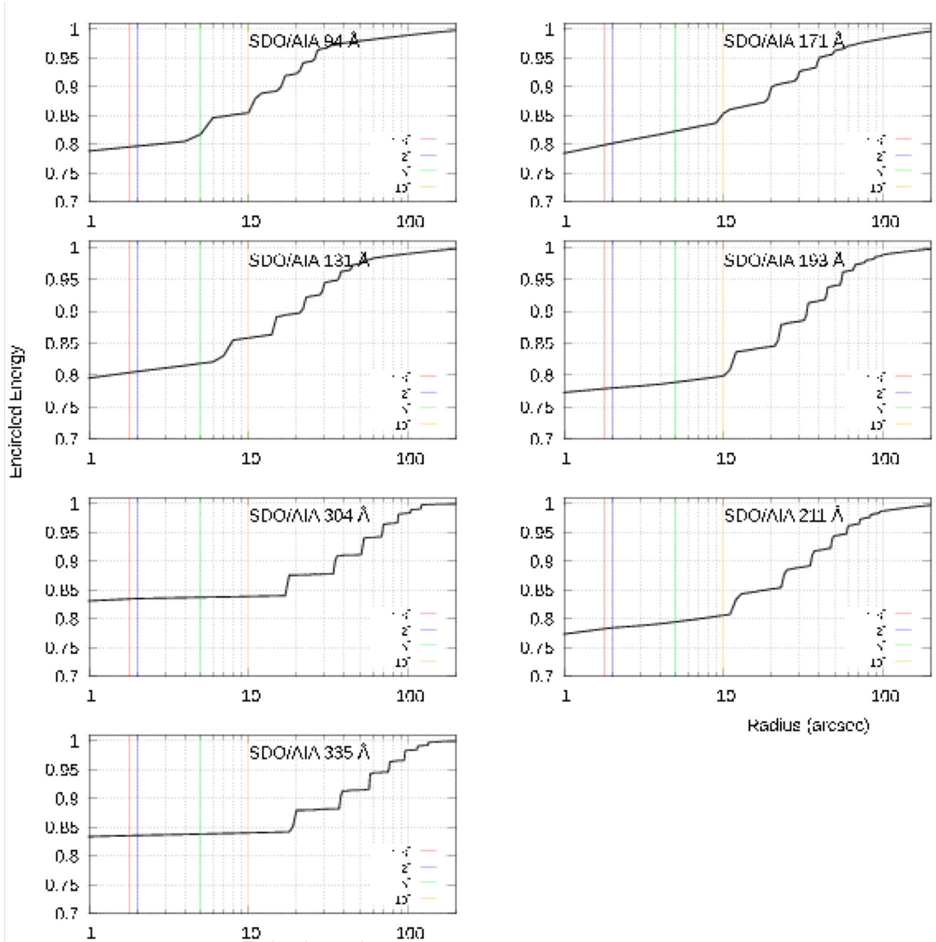

Encircled Energy

- Total energy (normalized to unity) in the PSF within a given radius.
- e.g. 94 Å: 79% of incident light arrives within 1" of its intended location; therefore, 21% of the incident light lands outside that distance. 85% of incident light falls within 10" of the intended location, while 15% falls further away.

ENCIRCLED ENERGY

- The nearly vertical steps are due to the spiky **diffraction** pattern.
- The sloping spaces between them are due to the smoothly modelled **scattering** portion of the PSF.
- 304 Å: stray light pattern is almost entirely due to observable diffraction pattern.
- 171 Å: has the highest proportion of scatter compared to diffraction.

Image normalized scatter

- Ratio of stray light to non-stray light, normalized to the non-scattered brightness in the core of the PSF.
- Estimate of the expected diffuse brightness in the image, given a measured brightness of well-focused features in the image.
- Computed the scatter at 2”, 5”,and 10” radii, normalized by that at a radius of 1.8”.

λ Å	Image normalized scatter 2”	5”	10”
94	27	25	19
131	26	23	18
304	20	20	19
335	20	19	19
171	27	23	20
193	29	28	26
211	29	27	25

APPLICATIONS – CONTRAST & PHOTOMETRY

EUV wavelengths 94, 131, 304, and 335 Å. On the disc.

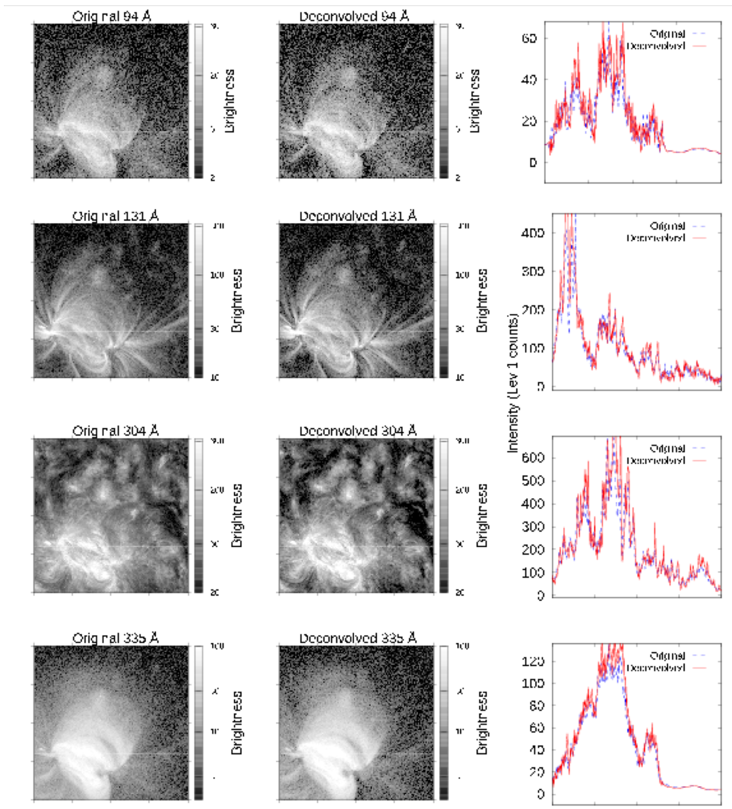

EUV wavelengths 171, 193, and 211 Å.

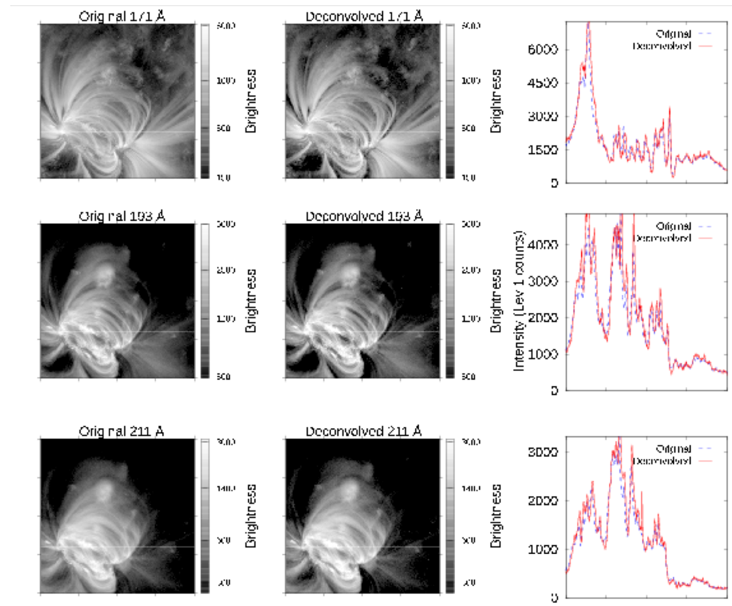

APPLICATIONS – CONTRAST & PHOTOMETRY

EUV wavelengths 94, 131, 304, and 335 Å. On the limb.

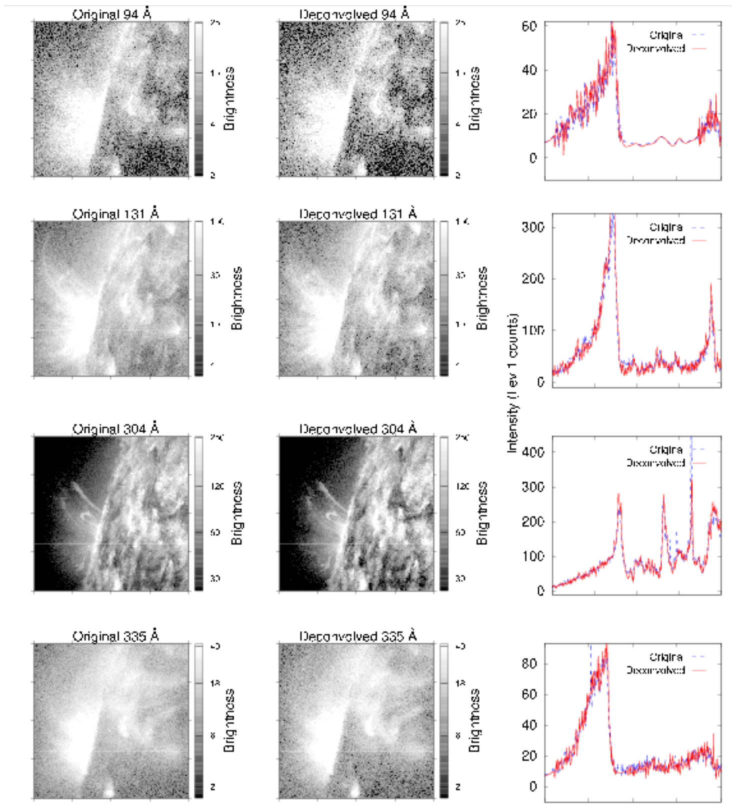

EUV wavelengths 171, 193, and 211 Å.

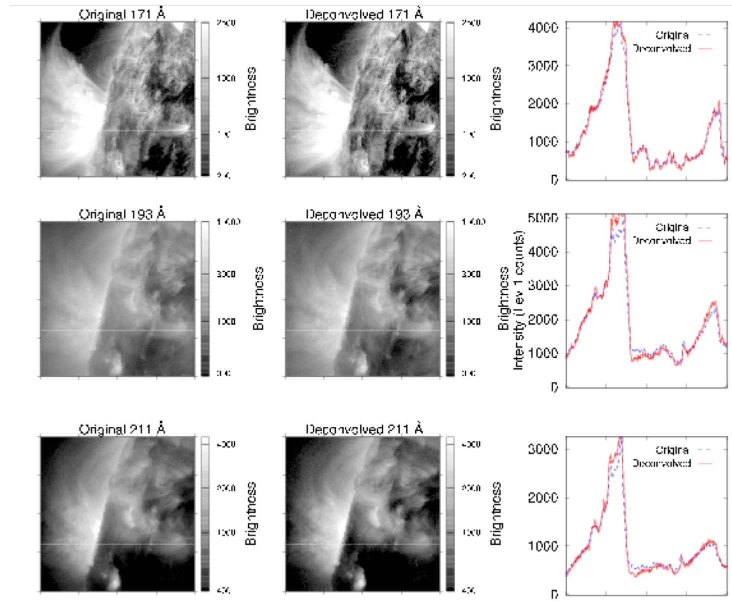

APPLICATIONS - DEM

Selected coronal loops. AIA image in 171 Å.

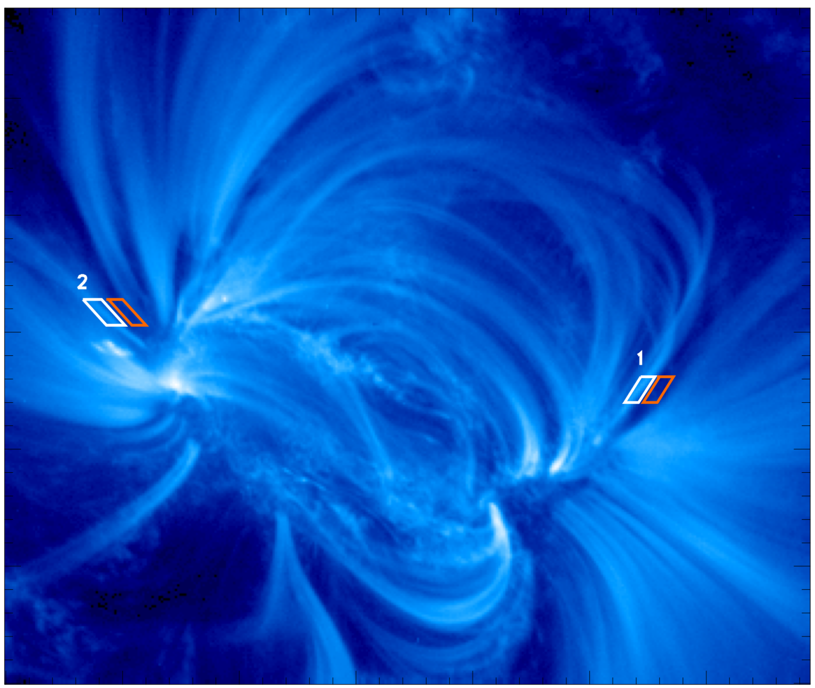

Schmelz and Pathak

DEM results. Left, middle: 50 Monte-Carlo realizations. Right: means (solid) and 1-σ error (dashed) at each temperature, original (black) and deconvolved (red).

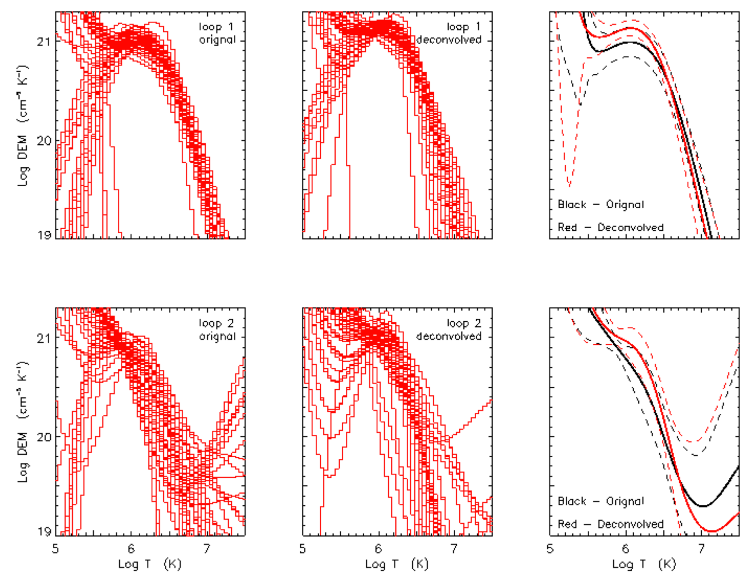

The means are within the 1-σ error. That is deconvolution alone is not significantly affecting the DEM results.

Concluding Remarks

- We determined the stray-light PSFs for all the EUV channels of the SDO/AIA telescope and generated their inverses; available online - http://psf.boulder.swri.edu.
- The PSFs consists of a diffraction kernel and an isotropic scattering term representing stray light.
- The inverse PSFs may be convolved directly with the respective Level-1 data to get the corrected images.
- Application of the PSFs improves the stray light performance by a factor of 10.
- Deconvolution significantly improves contrast; more visible in dark features such as miniature coronal holes.
- Deconvolution reduces the background haze significantly.
- Deconvolution alone does not affect DEM analysis of coronal loop segments, with appropriate background subtraction.

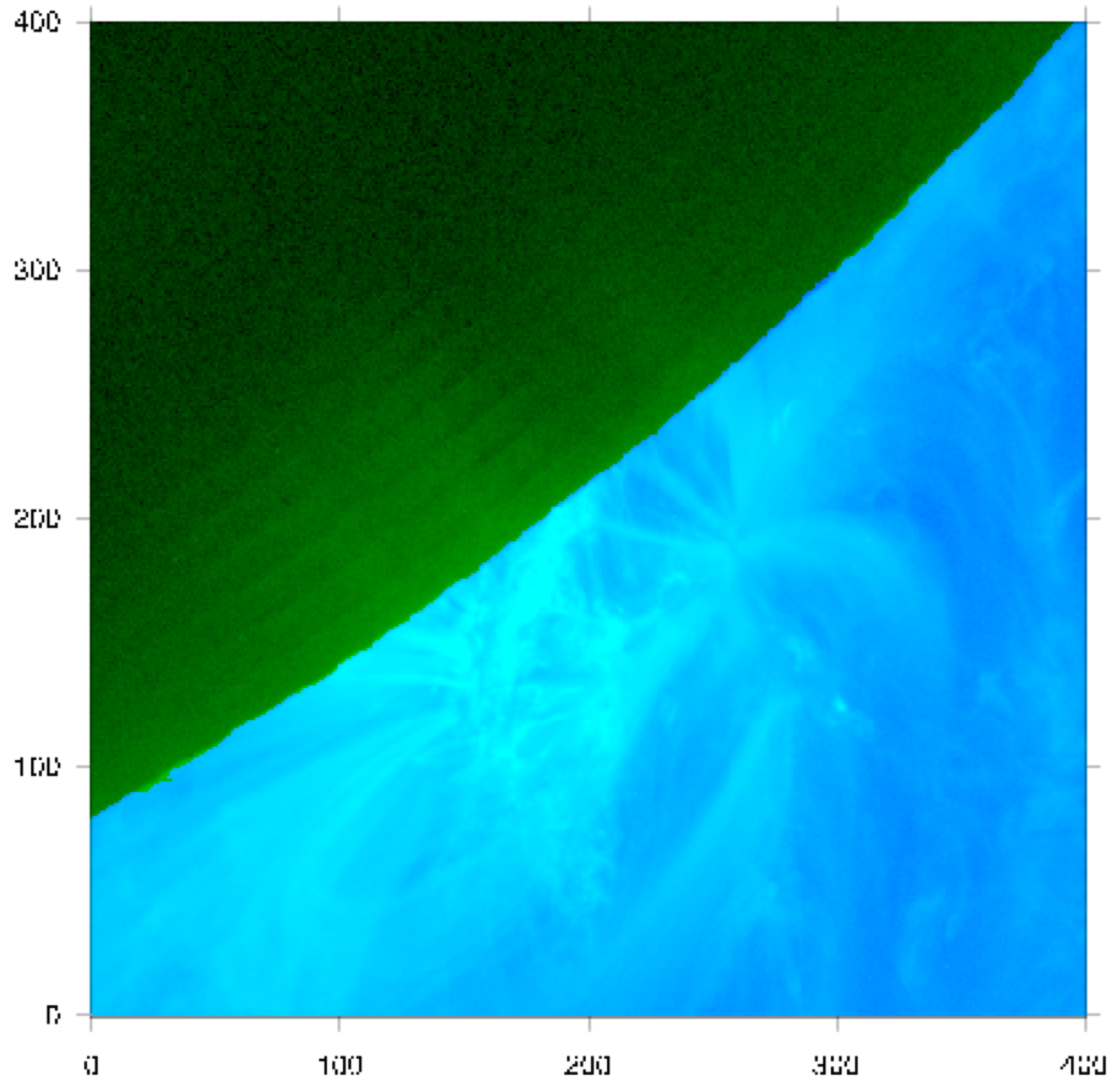
400
300
200
100
0
0
100
200
300
400

ARTIFACTS – LIMITATIONS OF DECONVOLUTION